

# Assessment of Urban Sprawl using Shannon Entropy Model, Oyo Metropolis, Oyo State, Nigeria

Alagbe Adedayo O.<sup>1</sup>, Effiong, E.<sup>2</sup>, Adeniyi Adebayo B<sup>1</sup>., Jimoh, A.O.<sup>2</sup>

<sup>1</sup>Department of Cartography & GIS, Federal School of Surveying, Oyo

<sup>2</sup>Department of Surveying & Geoinformatics, Federal School of Surveying, Oyo

Corresponding Author: [adedayoalagbe@gmail.com](mailto:adedayoalagbe@gmail.com)

## ABSTRACT

This study examines urban sprawl in Oyo metropolis, Nigeria, from 2000 to 2024, leveraging Geographic Information Systems (GIS) and remote sensing techniques to analyze land use and land cover changes. The goal was to evaluate urban expansion rates and patterns using Shannon's Entropy method. The methodology involved acquiring Landsat satellite images for the years 2000, and 2024, processing these images, and classifying them into three primary categories: Water Body, Urban Expansion, and Non-Urban Expansion. The results revealed a substantial increase in urban areas, growing from 1,731.58 hectares in 2000 to 11,932.50 hectares in 2024. This expansion has resulted in a decrease in non-urban areas and water bodies, indicating notable changes in land use and suburban development. Shannon's Entropy method quantified urban sprawl, showing dispersion increases with distance from the city center until a more compact growth pattern emerges. Specifically, entropy values indicated higher levels of sprawl in areas within 2700 meters from the city center, while beyond this range, the growth tended to be more contained. The study employed spatial queries and vector polygon conversion of classified imageries to facilitate precise calculations of affected areas. This comprehensive dataset is essential for understanding the spatial and temporal dynamics of urban sprawl in Oyo town. The findings underscore the necessity for implementing urban growth boundaries and promoting mixed-use development to achieve sustainable urban planning. Furthermore, the study emphasizes the importance of robust database management practices to maintain the integrity and reliability of spatial data, which are crucial for effective decision-making. This methodological approach and the insights gained can be applied to other regions experiencing similar urbanization trends, contributing to a broader understanding of urban sprawl dynamics and informing strategies for sustainable urban development.

Key Words: Shannon Entropy, Sprawl, Land use/Landcover, Urban area, Non-urban Area, Supervised Classification, GIS

## Study background

Rapid industrialization and economic growth in cities cause migration of population from rural to urban centers for employment and to improve their standard of living. As the migration rate increases, urban cities underwent major changes in land use and land cover which trigger several negative impacts such as overcrowding, water scarcity, air pollution, loss of productive agricultural lands and forest cover over the decades (Sridhar et al., 2020). In developing countries, rapid growth of urban population is one of the major challenges for governments and planning agencies (Sathianarayanan, 2019). Urbanization is the movement of rural residents to urban regions with subsequent population increases in urban regions. Urbanization is the result of socio-economic and political developments that lead to an expansion of big cities and changes in land use. Urban sprawl is simply a segment of urban growth. Urban sprawl is a global occurrence, and it attracts the attention of urban planners because of its nexus with the environmental efficiency of cities (Onilude & Vaz, 2021).

Global cities have undergone significant growth and transformation in recent decades, accompanied by substantial changes in land use. Urban growth monitoring and prediction play pivotal roles in understanding the evolving dynamics of urban landscapes, offering essential insights for sustainable urban development (Gilbert & Shi, 2024). As reported by the United Nations Department of Economic and Social Affairs, 54% of the global population, which amounts to roughly 3.9 billion individuals, currently live in urban areas. This figure is projected to increase to 6.3 billion by the year 2050, with almost 90% of future urban population growth expected to take place in cities within the developing world (Sathianarayanan, 2019). Despite urban areas occupying just 3% of the Earth's land surface, unplanned urbanization driven by population growth leads to significant environmental and socio-economic challenges. One prominent issue resulting from this is urban sprawl. Urban sprawl leads to issues such as poor economic conditions, inadequate drinking water quality, and sanitation problems for those living in slums and fringe areas (Rudra & Shikary, 2020).

The process of urban expansion in Oyo town is marked by the growth of unplanned settlements, which lack adequate services and infrastructure, and face environmental sanitation challenges (Rafiu et al., 2019). Sprawl is a multifaceted phenomenon that has both ecological and social impacts which leads to hazardous situations. This unpremeditated urbanization process has induced several hydrological impacts in terms of influencing the nature of surface runoff, erosion, encroachment in riparian zones, delivering pollutants to rivers, depletion of groundwater and other hydrological characteristics (Sridhar et al., 2020). Sprawl is a method of urbanization identified by low uniform densities. It is often uncoordinated and extends along the fringes of metropolitan areas with incredible speed. Land is often developed in a fragmented and piecemeal fashion, with much of the intervening space left vacant or in uses with little functionality. Urban sprawl often leads to excessive dependence on cars for accessing resources and community facilities (Torrens & Alberti, 2000).

Urban sprawl is a result of population concentration in urban centers (Shao et al., 2021). Urban sprawl leads to the absence of productive agricultural land, open green space, reduction of groundwater and loss of surface water bodies (Sridhar et al., 2020). Urban sprawl typically denotes the extensive expansion of housing, commercial development, and infrastructure over vast areas of land, often with minimal attention to urban planning principles (Shao et al., 2021).

The conventional topographical surveying and mapping techniques are expensive and time consuming for recognition of urban sprawl and its pattern (Sridhar et al., 2020). Urban planners and managers can now study and monitor urban conditions and growth using advanced geospatial technologies, a feat previously impossible (Shao et al., 2021).

Remote sensing is an inexpensive technology used for the investigation of urban sprawl these days. Geographical information systems (GIS) together with Remote sensing data are used for monitoring the emerging urbanization of the cities using digital satellite images and temporal data. From the earliest imagery (Landsat-MSS-1973) having more than 70m resolution to the present higher (IRS-P6 LISS-III) imageries having finer (5.8 m) resolution, it has been proved proficient in sensing the changes in land-cover and urban sprawl (Sridhar et al., 2020). Remote sensing technologies and satellite sensors have advanced urban geospatial monitoring and visual cognition research. Utilizing remote sensing data from various sources allows for an objective and scientific analysis of the spatio-temporal dimensions of urban development and changes in land use (Gilbert & Shi, 2024).

Remote sensing and GPS have enhanced the accuracy of measuring and analyzing urban sprawl. Several studies have applied remote sensing data and GIS techniques to provide information of land use transformation and degradation. To track deforestation, changes in cultivation, ecosystem and land use transformation patterns, airborne and satellite remote sensing are very precise and useful. Combining them with socioeconomic surveys, social sensing data, censuses, and other biophysical information collection methods have brought an improved understanding of land cover and use patterns and change detection as well as the factors driving these changes (Shao et al., 2021). This paper explores Shannon entropy method towards assessing the rate at which urban fringe has been expanding through years in Oyo metropolis.

## Methodology

### Study area

The history of Oyo dates to the 12th century when it was the headquarters of Oyo kingdom (Jimoh et al., 2018). Oyo is the ancient town in the southwest region of Nigeria and is located at an approximate coordinate of Latitudes 8° 25' and 9° 25' north of the equator and Longitudes 6° 45' and 7° 45' East of the Greenwich. Mabogunje (1976) identifies this area as the most suitable and favourable for human habitation and settlement development. There are three local government areas in Oyo town: Atiba, Oyo West and Oyo East Local Governments as shown in Figure 1. With the 2006 National Population Census, Oyo East Local Government has a population of 124,095, Oyo West Local Government with population figure of 136,457 and Atiba Local Government has a population of 168,246 (Jimoh et al., 2018). The area features hilly, dissected terrain with several peaks around 400m above sea level. The area is characterized by basement complex rocks underlying its geology. The annual mean temperature ranges between 25.8 and 30.2°C (c, 2005). Oyo town boasts a wide array of educational institutions, encompassing all levels from pre-primary schools to tertiary institutions. The prominent ones among the institutions are the Federal Government Girls College, Government Technical College, Emmanuel Alayande College of Education, Federal College of Education (Special), Federal School of Surveying, Ajayi Crowther University and Atiba University (Jimoh et al., 2018). Oyo is growing in infrastructure such as expanding road network, electricity, and drainage systems as well as facilities such

as hospitals, schools, filling stations, hotels, other social and recreational Centre's. Above all, there is the rapid development of various residential estates in the area.

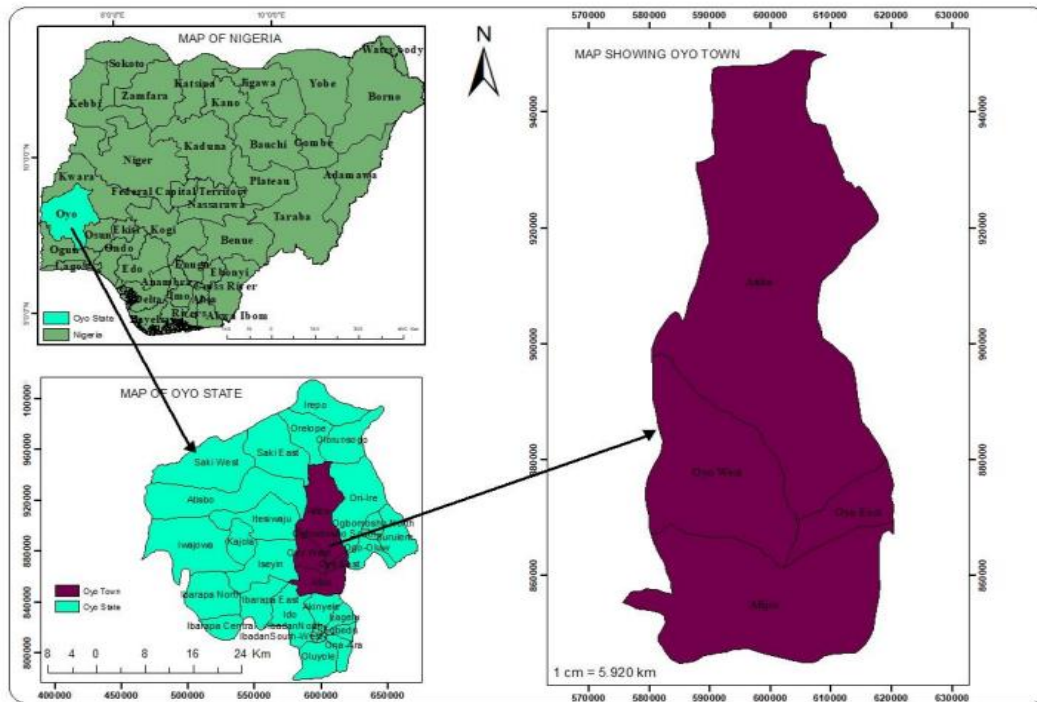


Figure 1: Location of the Study Area

### Data acquisition

This aspect deals with the sources of data used for this study. In academic research, various methodologies are employed to collect data. These methods fall into two categories namely: Primary data source and Secondary data source. Primary sources provide raw information and first-hand evidence. In this research, known ground points were picked using Handheld GPS to ensure that the supervised classification was accurate. Secondary data sources are data which already exists at the time of research. This study utilized Landsat satellite imagery from two distinct periods. These years were 2000 and 2024 respectively. The U.S. Geological Survey (USGS) provided these Landsat imageries. Google Earth provided a high-resolution image of the study area, aiding in supervised classification. The administrative map of the study area (Atiba, Oyo West, Oyo East and Afijio LGAs) were downloaded from Geographic infrastructure and Demographic data for Development (GRID<sup>3</sup>). The data were projected to Universal Transverse Mercator Projection to suit the needs of the project. Table 1 shows the description of Landsat Imageries used for the study.

Table 1: Description of Landsat Imageries used for the study

| Satellite Imagery | Landsat Sensor(s) | Date of Acquisition | Path | Row | Spatial Resolution |
|-------------------|-------------------|---------------------|------|-----|--------------------|
| 2000              | L7_ETM            | 2000-12-13          | 191  | 54  | 30                 |
| 2000              | L7_ETM            | 2000-12-13          | 191  | 55  | 30                 |
| 2024              | LANDSAT_9         | 2024-06-01          | 191  | 54  | 30                 |
| 2024              | LANDSAT_9         | 2024-06-01          | 191  | 55  | 30                 |

## Data processing

Landsat Satellite imageries from two different epochs were acquired for this study: 2000 and 2024. The data processing, classification and map embellishment were done in ArcGIS 10.7 environment. Composite bands of Landsat Imageries: Satellite imagery were captured in multiple wavelengths of reflected light otherwise known as image 'Bands'. These image bands were combined into one picture by displaying each band as either Red, Green or Blue. A satellite image mosaic was also carried out in this study. Every image represents a phase in a process. Combining a single image into a mosaic is straightforward and provides a clear overview for comparison. For the year 2000 and 2024, Landsat imageries were downloaded for Path 191 row 54 and path 191 row 55. These images were mosaicked together in ArcGIS 10.7 environment in order to form a single mosaicked image so that the extent of the study area would be covered. The mosaicked images for the years 2000 and 2024 are given in Figure 2. For this study, the administrative area of Oyo boundary was masked out of the mosaicked Landsat imageries 2000 2024 using the extract by mask tool in ArcGIS – Figure 3.

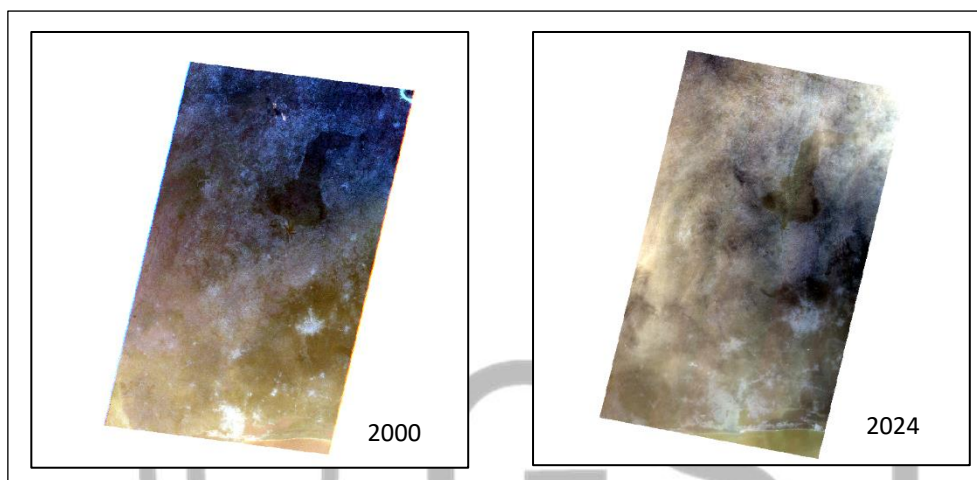


Figure 2: Mosaicked landsat image 2000 and 2024



Figure 3: Masked study area 2000 and 2024

Image Enhancement was also operationalized on the images in order to enhance the readability of the images for analysis. This was done through changing the resampling techniques, using the filtering tool and using the focal statistics tool.

## Data Analysis

### Supervised classification

For the urban sprawl of Oyo for the years 2000 and 2024, a classification scheme was developed. These included Water Body, Urban Expansion and Non-Urban Expansion. A classification scheme for the study area was created using prior knowledge, a quick survey, and information from past research. The established categorization method provides a very broad classification in which the land use land cover is identified by a single digit.

**Table 2: Classification Scheme Table**

| LAND COVER CLASS    | DEFINITION  |
|---------------------|---|
| Water body          | Rivers, streams   |
| Urban Expansion     | Cith growth and development of undeveloped areas.       |
| Non_Urban Expansion | Non-urban areas forests, parks, vegetation and farmland |

Supervised Image classification was performed using interactive Supervised Classification in ArcGIS 10.7 environment. After the supervised classification, accuracy assessment was carried out on the imageries. Thereafter Urban Expansion Intensity Index and Shannon Entropy Method followed. Figures 4 and 5 depicts the supervised classification for Landsat imageries 2000 and 2024.

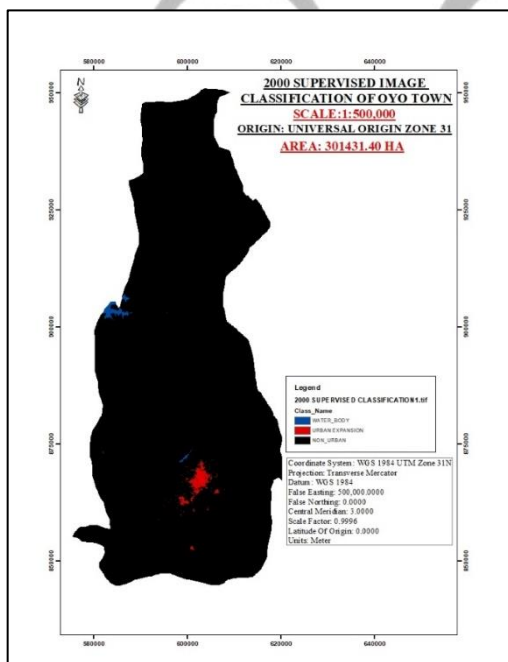


**Figure 4: Supervised classification 2000**

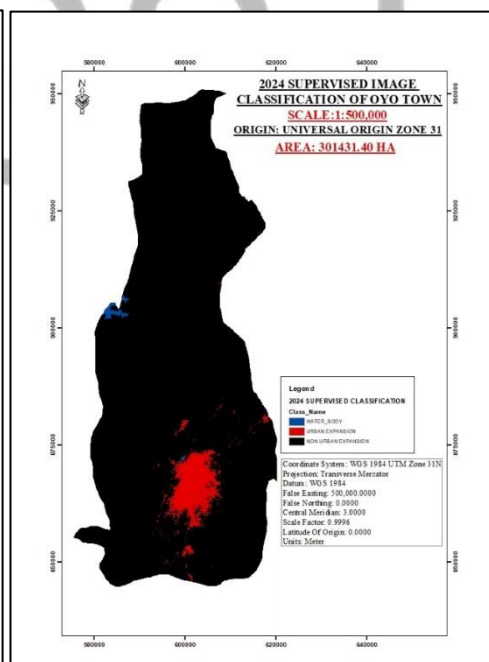


**Figure 5: Supervised classification 2024**

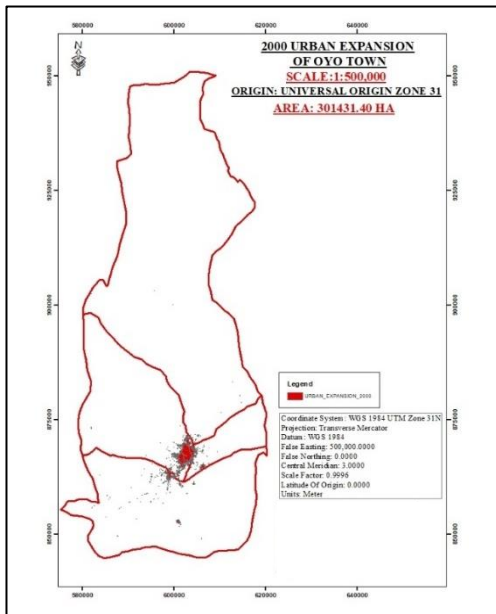


Figure 4: Urban Areas 2000

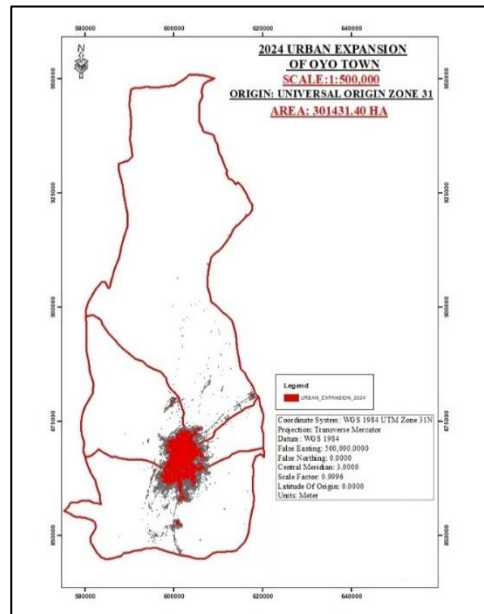


Figure 5: Non-Urban Areas 2024

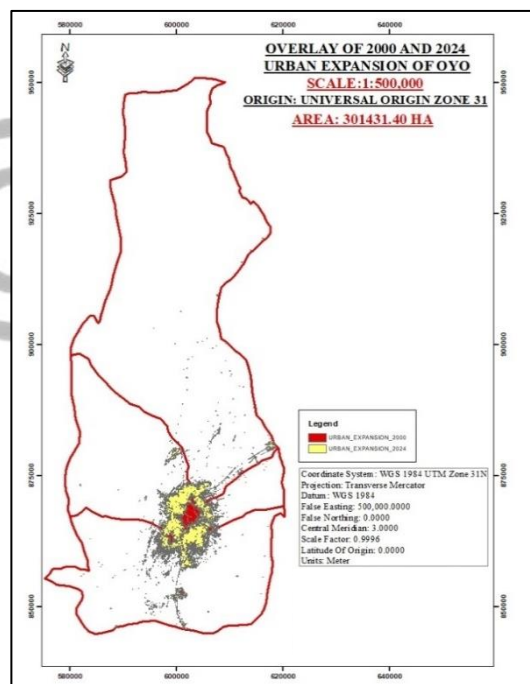


Figure 6: Overlay of Urban Expansion 2000 and 2024

### Land cover Inventory and Area calculation

The static land cover class distribution for each study year as derived from the analysis is presented in tables below

**Table 3: Landuse classification 2000**

| OBJECT ID | SHAPE   | CLASS_NAME          | AREA (SQM)    | AREA(HA)      |
|-----------|---------|---------------------|---------------|---------------|
| 1         | Polygon | Water Body          | 10423752.88   | 1042.375288   |
| 2         | Polygon | Urban Expansion     | 17315806.58   | 1731.580658   |
| 3         | Polygon | Non-Urban Expansion | 3014314040.17 | 301431.404017 |

**Table 4: Landuse classification 2024**

| OBJECT ID | SHAPE   | CLASS_NAME          | AREA (SQM)  | AREA(HA)    |
|-----------|---------|---------------------|-------------|-------------|
| 1         | Polygon | Water Body          | 9736601.64  | 973.660164  |
| 2         | Polygon | Urban Expansion     | 119325055.5 | 11932.50555 |
| 3         | Polygon | Non-Urban Expansion | 2912988586  | 291298.8586 |

### General change matrix

The general change matrix in percentage is given in Table 5

**Table 5: Change Matrix for years 2000 and 2024**

| LULC CLASS/YEARS    | 2000             |             | 2024               |             |
|---------------------|------------------|-------------|--------------------|-------------|
|                     | Area (HA)        | Area (%)    | Area (HA)          | Area (%)    |
| Water Body          | 1042.375288      | 0.342655135 | 973.660164         | 0.320067088 |
| Urban Expansion     | 1731.580658      | 0.569214381 | 11932.50555        | 3.922520865 |
| Non-Urban Expansion | 301431.404       | 99.08813048 | 291298.8586        | 95.75741205 |
| TOTAL               | <b>304205.36</b> | 100         | <b>304205.0243</b> | 100         |

### Assessment of nature, status, trend, rate and magnitude of changes

**Table 6: Land Cover Change: Magnitude, Trend, Rate and Direction (2000-2024)**

| Activity types      | Area Covered (km <sup>2</sup> ) |             | Difference (Ha) | Increase/Decrease% | Annual rate of increase or decrease % |
|---------------------|---------------------------------|-------------|-----------------|--------------------|---------------------------------------|
|                     | 2000                            | 2024        | 2000 - 2024     | 2000 - 2024        | 2000 - 2024                           |
| Water Body          | 1042.375288                     | 973.660164  | -68.715124      | 6.592167408        | 1.582120178                           |
| Urban Expansion     | 1731.580658                     | 11932.50555 | 10200.92489     | 589.1105819        | 141.3865397                           |
| Non-Urban Expansion | 301431.404                      | 291298.8586 | -10132.5454     | 3.361476364        | 0.806754327                           |

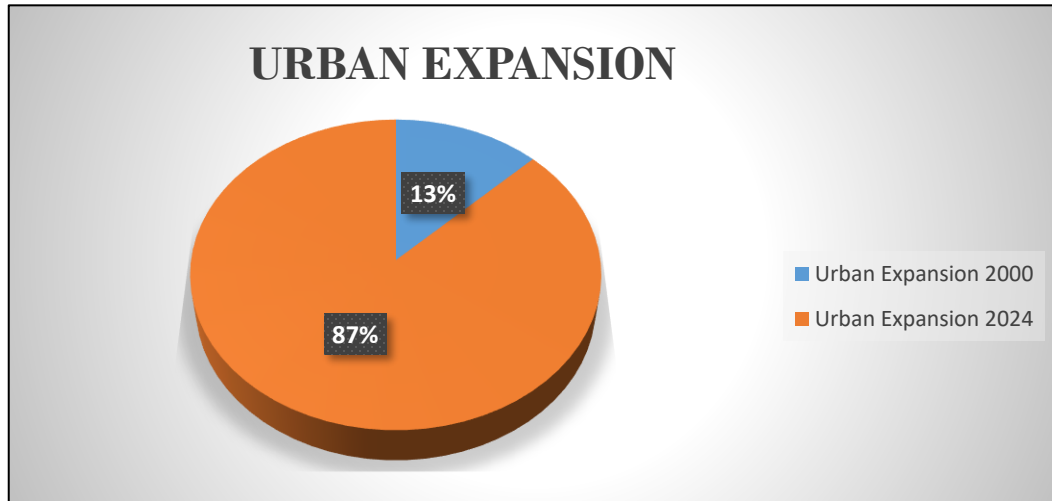


**Figure 7: Pie Chart for Urban Expansion years 2000 and 2024**

### Classification accuracy and error matrix

An accuracy assessment of a classified image provides information about the quality that can be obtained from remotely sensed data. Accuracy assessment is performed by comparing a map produced from remotely sensed data with another map obtained from some other source. Landscape often changes rapidly. Therefore, it is best to collect the ground reference as close to the date of remote sensing data acquisition as possible. Overall accuracy indicates the percentage of reference sites that were correctly mapped. Overall accuracy is given as a percentage, with 100% indicating perfect classification of all reference sites. Overall accuracy is the easiest to calculate and understand but ultimately only provides the map user and producer with basic accuracy information. The diagonal elements represent the areas that were correctly classified. To determine the overall accuracy, sum the number of correctly classified sites and divide this by the total number of reference sites. Kappa Coefficient is a statistical test in evaluating the accuracy of a classification. Kappa essentially evaluates how well the classification performed as compared to just randomly assigning values, i.e., did the classification do better than random. The Kappa Coefficient can range from -1 to 1. A value of 0 indicated that the classification is no better than a random classification. A negative number indicates the classification is significantly worse than random. A value close to 1 indicates that the classification is significantly better than random. The formula is given below

$$\text{Kappa Coefficient} = \frac{(\text{TS} * \text{TCS}) - \sum(\text{Col. tot} * \text{Row. tot})}{\text{TS}^2 - \sum(\text{Col. tot} * \text{Row. tot})}$$

Where;

TS = the number of rows in the error matrix

TCS = the number of columns in the error matrix

TS<sup>2</sup>= total number of observations included in matrix

Col.tot = total of observations in Column

Row.tot = total of observations in Row

**Table 7: Classification accuracy result table**

| Kappa     | Agreement |
|-----------|-----------|
| <0.20     | Poor      |
| 0.20-0.40 | Fair      |
| 0.41-0.60 | Moderate  |
| 0.61-0.80 | Good      |
| 0.81-1.00 | Very Good |

**Table 8: Pivot (2000-2024)**

| OBJECTID | FREQUENCY | True | PIVOT |
|----------|-----------|------|-------|
| 1        | 131       | 1    | 1     |
| 2        | 142       | 2    | 45    |
| 3        | 142       | 3    | 105   |

**Table 9: Frequency (2000-2024)**

| OBJECTID | PIVOT | True1 | True2 | True3 |
|----------|-------|-------|-------|-------|
| 1        | 1     | 131   | 0     | 0     |
| 2        | 45    | 0     | 142   | 0     |
| 3        | 105   | 0     | 0     | 142   |

**Table 10: Result table**

| CATEGORY          | WATER | URBAN | NON URBAN | TOTAL | USER ACCURACY |
|-------------------|-------|-------|-----------|-------|---------------|
| WATER             | 131   | 0     | 0         | 131   | 100%          |
| URBAN             | 0     | 142   | 0         | 142   | 100%          |
| NON URBAN         | 0     | 0     | 142       | 142   | 100%          |
| TOTAL             | 131   | 142   | 142       | 415   |               |
| PRODUCER ACCURACY | 100%  | 100%  | 100%      |       |               |

**Table 11: KAPPA Coefficient (2000)**

| TS  | TCS | TS*TCS | $\sum(\text{Col.tot}*\text{Row.tot})$ | $\text{TS}*TCS-\sum$ | TS^2   | TS^2- $\sum$ | KAPPA      |
|-----|-----|--------|---------------------------------------|----------------------|--------|--------------|------------|
| 415 | 415 | 172225 | 57489                                 | 114736               | 172225 | 114736       | <b>0.9</b> |

**Table 12: Pivot Table (2024)**

| OBJECTID | FREQUENCY | TRUE | PREDICT |
|----------|-----------|------|---------|
| 1        | 57        | 1    | 1       |
| 2        | 113       | 2    | 21      |
| 3        | 51        | 3    | 155     |

**Table 13: Frequency (2024)**

| OBJECTID | PREDICT | TRUE1 | TRUE2 | TRUE3 |
|----------|---------|-------|-------|-------|
| 1        | 1       | 57    | 0     | 0     |
| 2        | 21      | 0     | 113   | 0     |
| 3        | 155     | 0     | 0     | 51    |

**Table 14: Result (2024)**

| CATEGORY          | WATER | URBAN | NON URBAN | TOTAL | USER ACCURACY |
|-------------------|-------|-------|-----------|-------|---------------|
| WATER             | 57    | 0     | 0         | 57    | 100%          |
| URBAN             | 0     | 113   | 0         | 113   | 100%          |
| NON URBAN         | 0     | 0     | 51        | 51    | 100%          |
| TOTAL             | 57    | 113   | 51        | 221   |               |
| PRODUCER ACCURACY | 100%  | 100%  | 100%      |       |               |

**Table 15: KAPPA Coefficient (2024)**

| TS  | TCS | TS*TCS | Σ(Col.tot*Row.tot) | TS*TCS-Σ | TS^2  | TS^2-Σ | KAPPA |
|-----|-----|--------|--------------------|----------|-------|--------|-------|
| 221 | 221 | 48841  | 18619              | 30222    | 48841 | 30222  | 1     |

**Urban expansion intensity index**

The urban expansion intensity index (UEII) is the ratio of the change in urban land area in a unit of time to the total land area in a spatial unit. In other words, it quantifies the change in a built-up area between different given points in time as a proportion of the total area of the landscape. UEII is computed using the equation below:

$$UEII = \frac{ULALB - ULALA}{t} / ULAi * 100$$

Where;

UEII is the changing intensity for a given time interval

ULALB - ULALA is the area of land change from non-built-up to built-up during the given time interval

TLAi is the area of the entire landscape; a

t is the time span of the given time interval.

**Table 16: Urban Intensity Index summary table**

| Value range  | Inference       |
|--------------|-----------------|
| 0 to 0.28    | Slow            |
| 0.28 to 0.59 | Low speed       |
| 0.59 to 1.05 | Medium speed    |
| 1.05 to 1.92 | High speed      |
| >1.92        | Very high speed |

| CLASS                     | YEAR 2000 (SQM)   | YEAR 2024 (SQM)   |
|---------------------------|-------------------|-------------------|
| NON URBAN EXPANSION       | 3014314040        | 2912988586        |
| URBAN EXPANSION           | 17315806.58       | 119325055.5       |
| WATER BODY                | 10423752.88       | 9736601.64        |
| <b>TOTAL AREA</b>         | <b>3042053600</b> | <b>3042050244</b> |
| CLASS                     | YEAR 2000 (SQM)   | YEAR 2024 (SQM)   |
| NON URBAN EXPANSION       | 3024737793        | 2922725188        |
| URBAN EXPANSION           | 17315806.58       | 119325055.5       |
| <b>TOTAL AREA</b>         | <b>3042053600</b> | <b>3042050244</b> |
| <b>TOTAL AREA AVERAGE</b> | <b>3042051922</b> |                   |
| <b>TIME PERIOD</b>        | <b>24</b>         |                   |

Table 17: Urban Intensity Index calculation

Table 18: Urban Intensity Index

| ULALB       | ULALA       | ULALB - ULALA | t  | ULALB - ULALA/t | TLAi       | ULALB - ULALA/t/TLAi | UEII         |
|-------------|-------------|---------------|----|-----------------|------------|----------------------|--------------|
| 119325055.5 | 17315806.58 | 102009249     | 24 | 4250385.374     | 3042051922 | 0.00139721           | <b>0.14%</b> |

**Shannon Entropy Method**

The image processing and classification in geographical information system and the remote sensing combined with statistical methods like Shannon entropy can be used to analyze, and detect urban expansion and sprawling. Shannon is a widely used to study urban sprawl phenomenon as a favorable measure of spatial dispersion or concentration. Entropy is an efficient technique for comparing urban sprawl patterns, therefore, the Shannon’s entropy for each zones and time period must be calculated, and the degree of sprawl can be measured by the value of entropy which varies from 0 to logarithm of number of zones or time period. The formula for the relative entropy is given by:

$$Hn = \sum_i^n Pi \log e \left( \frac{1}{pi} \right)$$

where;

Pi = Proportion of the built-up areas in the ith zone.

n = Total number of zones.

**Relative Entropy (RE)** is defined as the measure of the degree of randomness of any geographical variable (i.e., urban growth). It is an effective indicator to evaluate the patterns of urban growth, whether compact or dispersed. However, by dividing calculated absolute Shannon’s entropy by ln(n), one can get the relative Shannon’s entropy. The relative Shannon’s entropy always varying between 0 to 1 values which gives clearer understanding about the sprawl

$$Hn = \sum_i^n Pi \log e \left( \frac{1}{pi} \right) / \log_e(n)$$

where;

Pi = Proportion of the built-up areas in the ith zone.

n = Total number of zones.

The rate of urban change for the years 2000 and 2024 is given by

$$H_n(t_2) - H_n(t_1)$$

The more compact of the structures and the built up areas is closer to zero entropy value, while the closer to the logarithm number of zones is the more dispersed the region. The rate of urban change relative entropies is given in the Table 4.8 below

**Table 19: Relative entropy summary result table**

| Relative Entropy |                        |
|------------------|------------------------|
| Near 0           | Compact distribution   |
| Near 1           | Dispersed distribution |

In order to calculate the absolute and relative entropies for urban sprawl in Oyo for the periods 2000 and 2024. The urban areas were divided into five zones each at an interval of 2000m, 4000m, 6000m, 8000m and 15000m respectively for years 2000 and 2024. Figures 4.12 and Figure 4.13 show the buffer circles around the city center for the years.

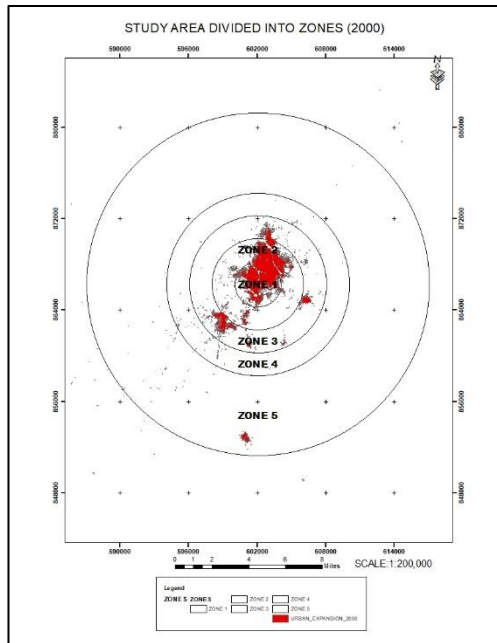


Figure 8: Buffer Cycles center (2000)

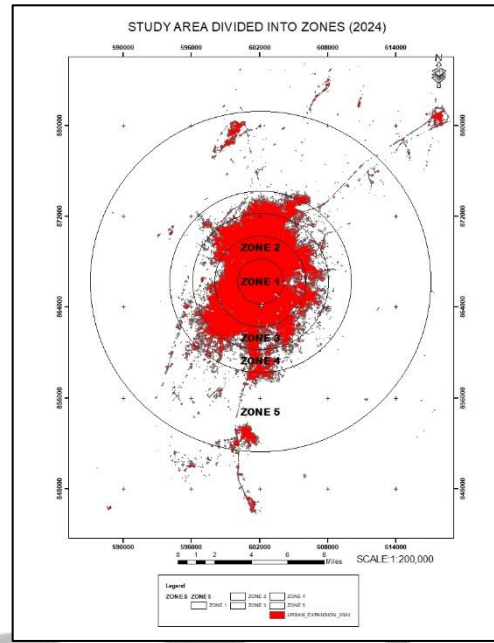


Figure 9: Buffer Cycles center (2024)

Table 20: Buffer zones for year 2000

| CLASS             | ZONE 1      | ZONE 2      | ZONE 3      | ZONE 4      | ZONE 5      |
|-------------------|-------------|-------------|-------------|-------------|-------------|
| <b>NON-URBAN</b>  | 4562613.13  | 36787109.6  | 96299975.34 | 183293950.1 | 688654562   |
| <b>URBAN</b>      | 8002924.23  | 13466225.33 | 16691417.73 | 16805655.96 | 17238531.29 |
| <b>WATER BODY</b> | 0           | 10477.36    | 103437.22   | 958979.95   | 958979.95   |
| <b>TOTAL</b>      | 12565537.36 | 50263812.29 | 113094830.3 | 201058586   | 706852073.2 |

Table 21: Absolute entropy calculation for year 2000

| YEAR        | ZONE | TOTAL AREA | BUILT_UP | Pi          | I/Pi            | Ln(I/Pi)    | Pi*Ln(I/Pi) |
|-------------|------|------------|----------|-------------|-----------------|-------------|-------------|
| <b>2000</b> | 1    | 12565537   | 8002924  | 0.636894707 | 1.570118247     | 0.451150933 | 0.287335641 |
|             | 2    | 50263812   | 13466225 | 0.267910943 | 3.732583635     | 1.317100657 | 0.352865679 |
|             | 3    | 113094830  | 16691418 | 0.147587805 | 6.775627578     | 1.913331994 | 0.282384469 |
|             | 4    | 201058586  | 16805656 | 0.083585866 | 11.96374521     | 2.481880844 | 0.207450159 |
|             | 5    | 706852073  | 17238531 | 0.024387749 | 41.00419353     | 3.713674343 | 0.09056816  |
|             |      |            |          |             | <b>ABSOLUTE</b> |             | 1.220604107 |

**Table 22: Relative entropy calculation for year 2000**

| YEAR | ZONE | TOTAL AREA | BUILT_UP | Pi       | I/Pi     | Ln(I/Pi) | Pi*Ln(I/Pi) | (Pi*Ln(I/Pi))/ln(n) |
|------|------|------------|----------|----------|----------|----------|-------------|---------------------|
| 2000 | 1    | 12565537   | 8002924  | 0.636895 | 1.570118 | 0.451151 | 0.2873356   | 0.178531672         |
|      | 2    | 50263812   | 13466225 | 0.267911 | 3.732584 | 1.317101 | 0.3528657   | 0.219247773         |
|      | 3    | 113094830  | 16691418 | 0.147588 | 6.775628 | 1.913332 | 0.2823845   | 0.175455335         |
|      | 4    | 201058586  | 16805656 | 0.083586 | 11.96375 | 2.481881 | 0.2074502   | 0.128896031         |
|      | 5    | 706852073  | 17238531 | 0.024388 | 41.00419 | 3.713674 | 0.0905682   | 0.056273161         |
|      |      |            |          |          |          |          | RELEATIVE   | 0.758403973         |

**Table 23: Buffer zones for year 2024**

| CLASS      | ZONE 1      | ZONE 2      | ZONE 3      | ZONE 4      | ZONE 5      |
|------------|-------------|-------------|-------------|-------------|-------------|
| NON-URBAN  | 63572.84    | 2330075.49  | 25158983.39 | 94840683.12 | 688654562   |
| URBAN      | 12501964.53 | 47933736.79 | 87935846.9  | 105539324   | 17238531.29 |
| WATER BODY | 0           | 0           | 0           | 678578.93   | 678578.93   |
| TOTAL      | 12565537.37 | 50263812.28 | 113094830.3 | 201058586   | 706571672.2 |

**Table 24: Absolute entropy calculation for year 2024**

| YEAR | ZONE | TOTAL AREA | BUILT_UP  | Pi          | I/Pi        | Ln(I/Pi)    | Pi*Ln(I/Pi) |
|------|------|------------|-----------|-------------|-------------|-------------|-------------|
| 2024 | 1    | 12565537   | 12501965  | 0.994940699 | 1.005085028 | 0.005072143 | 0.005046481 |
|      | 2    | 50263812   | 47933737  | 0.953643081 | 1.048610345 | 0.047465807 | 0.045265438 |
|      | 3    | 113094830  | 87935847  | 0.777540818 | 1.286106113 | 0.251619137 | 0.19564415  |
|      | 4    | 201058586  | 105539324 | 0.524918264 | 1.905058498 | 0.644512716 | 0.338316496 |
|      | 5    | 706571672  | 17238531  | 0.024397428 | 40.98792759 | 3.713277574 | 0.090594421 |
|      |      |            |           |             |             | ABSOLUTE    | 0.674866986 |

**Table 25: Relative entropy calculation for year 2024**

| YEAR | ZONE | TOTAL AREA | BUILT_UP  | Pi       | I/Pi     | Ln(I/Pi) | Pi*Ln(I/Pi) | (Pi*Ln(I/Pi))/ln(n) |
|------|------|------------|-----------|----------|----------|----------|-------------|---------------------|
| 2024 | 1    | 12565537   | 12501965  | 0.994941 | 1.005085 | 0.005072 | 0.0050465   | 0.003135555         |
|      | 2    | 50263812   | 47933737  | 0.953643 | 1.04861  | 0.047466 | 0.0452654   | 0.028124998         |
|      | 3    | 113094830  | 87935847  | 0.777541 | 1.286106 | 0.251619 | 0.1956441   | 0.121560545         |
|      | 4    | 201058586  | 105539324 | 0.524918 | 1.905058 | 0.644513 | 0.3383165   | 0.210207858         |
|      | 5    | 706852073  | 17238531  | 0.024388 | 41.00419 | 3.713674 | 0.0905682   | 0.056273161         |
|      |      |            |           |          |          |          | RELATIVE    | 0.419302117         |

### Discussion of results

Figures 4 and 5 shows the classified Landsat images of Oyo town for the year 2000 and 2024. The classified imageries show that Oyo had grown in its urban areas in year 2024. The area calculation was given in Table 3 and Table 4. In Table 5 for the year 2000, water Body occupies 1042.375 Ha (0.342%), Urban Expansion 1731.58 Ha (0.5692%), and Non-urban Expansion 301431 Ha (99.08%). In 2024, Water Body occupies 973.66Ha (0.32%), Urban Expansion

11932.50 (3.9225%), and Non-Urban Expansion 291298,85 Ha (95.75%). Statistical tables was depicted in form of pie charts to compare the urban areas in 2000 and urban areas in 2024. It is clear in the table 5 that within the 24 years period, Water Body changes to 68.715124 Ha representing 6.592 decrease at 1.5821% annual rate of change. Urban Expansion changes to 10200.924 Ha representing 589.110% increase at 141.38% annual rate of change, while Non-Urban Expansion assumes a change of 10132.54 Ha representing 3.3614 decrease at the rate of 63.567% annually. In this study, after the Landsat imageries 2000 and 2024 were classified, we proceeded towards performing an accuracy assessment in order to compare the relationship between known reference data (ground data) and the corresponding results obtained from classification. In Table 11, the Kappa Coefficient for the supervised classification 2000 was 0.9 which falls within the agreement 0.81-1.00. This means that the relationship between known reference data (ground data) and the corresponding results obtained from classification for the year 2000 was very good. Also, for the year 2024 in Table 14, the Kappa Coefficient for the supervised classification was 1 which falls within the agreement 0.81-1.00. This means that the relationship between known reference data (ground data) and the corresponding results obtained from classification for the year 2000 was very good. Urban Exanion Intensity Index (UEII) was among the key indicators used to examine urban expansion from the perspective of non-urban to urban conversion in Oyo Metropolis. Additionally, UEII was employed to recognize the preferences of urban growth and to compare the speed or intensity of land use changes in Oyo Metropolis. The urban expansion intensity index used in the quantitative characteristics of urban expansion over different study periods of 2000 and 2024 was given by 0.14. The value 0.14 is an indication that the rate of non-urban areas converting to urban areas is slow. Most urbanization had taken place around Oyo metropolis. Tables 19 to Table 25 shows that calculation for the entropy values (absolute and relative) for the years 2000 and 2024. In Table 21 and Table 22, 1.220604107 and 0.674866986 respectively gave the absolute entropy for the year 2000 and 2024. The absolute entropy value for the year 2000 is an indication that there was more dispersed distribution since the value is closer to one. Most of the urban areas in the year 2024 shows some more dispersion than compactness of distribution of urban areas. This is evident in the absolute value for year 2024 which is close to zero but closer to one. The relative Shannon's entropy always varying between 0 to 1 value which gives clearer understanding about the sprawl. The difference of the relative entropies was 0.33910 which is closer to zero than one. Hence urban distribution in Oyo town indicates that there is currently more compact distribution.

## Conclusion

The study successfully highlighted the significant urban sprawl in Oyo from 2000 to 2024, providing valuable insights into the dynamics of land use and land cover changes. The dramatic increase in urban areas and the corresponding decrease in non-urban areas and water bodies reflect substantial environmental and social transformations. These changes underscore the need for effective urban planning and management strategies to address the challenges associated with rapid urbanization. The use of GIS and remote sensing techniques proved effective in analyzing and visualizing urban sprawl. The supervised classification approach, coupled with the Shannon Entropy Method, provided a detailed and comprehensive analysis of the spatial distribution and concentration of urban growth. This methodological approach can be applied to other regions experiencing similar urbanization trends, contributing to a broader understanding of urban sprawl dynamics. Database management emerged as a critical aspect of the study, highlighting the importance of data security, integrity, and maintenance. Reliable spatial data are essential for informed decision-making and effective urban planning. The recommendations for database management practices provided in this study can serve as guidelines for future research and applications in the field of spatial information management.

## References

- Gilbert, K. M., & Shi, Y. (2024).** Urban Growth Monitoring and Prediction Using Remote Sensing Urban Monitoring Indices Approach and Integrating CA-Markov Model: A Case Study of Lagos City, Nigeria. *Sustainability*, 16(1), Article 1. <https://doi.org/10.3390/su16010030>
- Jimoh, R., Afonja, Y., Albert, C., & Amoo, N. (2018).** Spatio-Temporal Urban Expansion Analysis in a Growing City of Oyo Town ,Oyo State, Nigeria Using Remote Sensing And Geographic Information System (GIS) Tools. *International Journal of Environment and Geoinformatics*, 5(2), 104–113.

- Onilude, O. O., & Vaz, E. (2021).** Urban Sprawl and Growth Prediction for Lagos Using GlobeLand30 Data and Cellular Automata Model. *Sci*, 3(2), Article 2. <https://doi.org/10.3390/sci3020023>
- Rudra, S., & Shikary, C. (2020).** Measuring Urban Land Use Change and Sprawl Using Geospatial Techniques: A Study on Purulia Municipality, West Bengal, India. *Journal of the Indian Society of Remote Sensing*, 48. <https://doi.org/10.1007/s12524-020-01212-6>
- Sathianarayanan, M. (2019).** Spatial and Temporal Dynamics of Urban Sprawl Using Multitemporal Images and Relative Shannon Entropy Model in Adama. 48–57. <https://doi.org/10.24321/2455.3190.201801>
- Shao, Z., Sumari, N. S., Portnov, A., Ujoh, F., Musakwa, W., & Mandela, P. J. (2021).** Urban sprawl and its impact on sustainable urban development: A combination of remote sensing and social media data. *Geo-Spatial Information Science*, 24(2), 241–255. <https://doi.org/10.1080/10095020.2020.1787800>
- Sridhar, M. B., Sathyanathan, R., Subramani, R., & Sudalaimathu, K. (2020).** Urban Sprawl Analysis Using Remote Sensing Data And Its Impact On Surface Water Bodies: Case Study Of Surat, India. *IOP Conference Series: Materials Science and Engineering*, 912(6), 062070. <https://doi.org/10.1088/1757-899X/912/6/062070>
- Torrens, P. M., & Alberti, M. (n.d.).** Measuring Sprawl.

